Available online at www.sciencedirect.com
ScienceDirect
Journal of the European Ceramic Society 29 (2009) 59–66
www.elsevier.com/locate/jeurceramsoc

Alumina-based nanocomposites obtained by doping with inorganic salt solutions: Application to immiscible and reactive systems

Paola Palmero [a,*], Valentina Naglieri [a], Jérôme Chevalier [b], Gilbert Fantozzi [b], Laura Montanaro [a]

[a] *Dept. SMIC, Politecnico of Torino, INSTM, R.U. PoliTO, LINCE Lab., Corso Duca degli Abruzzi, 24-10129 Torino, Italy*
[b] *Université de Lyon, INSA de Lyon, MATEIS UMR CNRS 5510, Bât. Blaise Pascal, 7 Av. Jean Capelle, 69621 Villeurbanne, France*

Received 9 November 2007; received in revised form 23 May 2008; accepted 30 May 2008
Available online 30 July 2008

Abstract

Doping of commercial alumina nanopowders by using aqueous solutions of metal salts was exploited to prepare alumina-based nanocomposites.

The same procedure was applied to produce a composite made of immiscible phases, that is an alumina–zirconia material, by doping an α-alumina powder with a zirconium chloride solution, as well as to produce an alumina–YAG (yttrium aluminium garnet) system by doping alumina with a yttrium chloride solution and promoting YAG formation by solid-state reaction at high temperature.

For this latter case, the difference in reactivity between two commercial powders, one made of transition alumina, the other of pure α-phase, was investigated in terms of phase evolution and purity.

In all cases natural sintering was performed to develop dense bodies.

Keywords: Al_2O_3–ZrO_2; Al_2O_3–YAG; Nanocomposites; Powder solid-state reactions; Sintering

1. Introduction

Ceramic nanocomposites can be prepared by using various processing routes starting from nanopowder mixing[1–3] or from nanocomposite powders obtained by co-precipitation of complex compositions.[4–8] Recently, the post-doping of an α-alumina powder by using a zirconium alkoxide and yttrium methoxyethoxide has been successfully exploited to prepare alumina–zirconia and alumina–yttrium aluminium garnet (YAG) micro-nanocomposite materials.[9–11] The precipitation of YAG particles at alumina grain boundaries and at multiple grain junctions, when an alumina matrix was doped with a yttrium salt, was already observed in the literature.[12–15] However, previous papers were mostly devoted to investigate the influence of a low yttrium content on the densification, grain growth[12,16] and creep behaviour of α-Al_2O_3,[14,17] as a result of yttrium segregation at alumina grain boundaries.[14,18,19]

This paper deals with the preparation of alumina-based nanocomposites following a doping procedure of alumina powders, but exploiting aqueous solutions of inorganic metal salts as dopant sources, to develop a metal oxide second-phase.

Two different systems were investigated. The first composite material, made of immiscible oxides, that is 95 vol.% alumina and 5 vol.% zirconia, was prepared by doping a commercial α-alumina powder with a zirconium chloride solution and subsequent drying and calcination to promote zirconia formation. For this composite, pure α-alumina was used as a starting powder to avoid the well-known problems connected with phase transformation of transition alumina and the resulting vermicular structure during high-temperature treatment.[20,21]

In contrast, in the case of 95 vol.% alumina–5 vol.% YAG nanocomposites, obtained by doping an alumina powder with a yttrium salt, since a solid-state reaction step is involved during calcination to yield the YAG phase, the behaviour of both doped transition and α-alumina nanopowders was investigated in terms of phase evolution and purity.

The microstructures of pressureless sintered bodies were finally characterized to study phases and grain size distribution.

* Corresponding author. Tel.: +39 0115644678; fax: +39 0115644699.
E-mail address: paola.palmero@polito.it (P. Palmero).

0955-2219/$ – see front matter © 2008 Elsevier Ltd. All rights reserved.
doi:10.1016/j.jeurceramsoc.2008.05.047

2. Experimental

2.1. An immiscible system: Al_2O_3–ZrO_2

A commercial α-alumina powder (TM-DAR TAIMICRON, supplied by Taimei Chemicals Co., Japan) was used to develop a 95 vol.% alumina and 5 vol.% zirconia nanocomposite. It is characterized by a mean particle size of 350 nm.[22]

Firstly, the alumina powder was dispersed in distilled water under magnetic stirring for 96 h or by ball-milling for 3 h by using α-alumina spheres (powder/spheres weight ratio of 1:10), in order to reach a similar particle size distribution in the dispersed slurries. During dispersion, an almost constant pH value of about 5.8 was reached.

Then, an aqueous solution of zirconium chloride (0.38 M) was drop-wise added to the alumina slurry (solid content of 33 wt.%) in a suitable amount to develop the above composition after calcination. After homogenization under stirring for 1 h, the doped suspensions were diluted down to 4 wt.% and dried by comparing two routes, precisely slow drying in oven at 105 °C and spray drying (Mini Spray Dried Büchi B-290).

The dried powders were calcined at 400, 500, 800, 1200 and 1500 °C (without soaking time at the maximum temperature) and at 1500 °C for 3 h, and then submitted to X-ray diffraction (XRD, Philips PW 1710) to investigate ZrO_2 crystallization. On the ground of XRD data, as-dried powders were pre-treated at 500 °C (without soaking time), uniaxially pressed into bars of 17 mm × 5 mm × 5 mm at about 300 MPa and finally sintered in a dilatometer (Netzsch 402E).

2.2. A reactive system: Al_2O_3–YAG

Two commercial alumina powders were used in this case: an α-alumina powder (Taimei, TM-DAR TAIMICRON) already described in the previous section, and a nanocrystalline transition alumina powder (NanoTek®, supplied by Nanophase Technologies, USA) prepared by physical vapor synthesis (PVS). This latter is characterized by an average crystallite size of about 47 nm[23] and it transforms into α-phase at about 1300 °C. However, a recent paper[24] has assessed that powder processing should induce a not negligible lowering of the above transformation temperature.

Post-doping was performed in order to develop 95 vol.% alumina–5 vol.% YAG composites (AY95), by reaction of the yttrium oxide precursor and a part of the alumina powder.

Taimei powder dispersion has been already described above. NanoTek powder was firstly dispersed in pure distilled water (solid content of 33 wt.%) and maintained under magnetic stirring for 120 h or by ball-milling for 2.5 h by using alumina spheres (powder/spheres weight ratio of 1:10), to obtain a similar particle size distribution in the final slurries. An almost constant pH value of about 5.5 was measured.

A $YCl_3{\cdot}6H_2O$ aqueous solution (0.3 M) was then added to the dispersed suspensions and maintained under magnetic stirring for 2 h. Powder suspensions diluted down to 4 wt.% were then spray-dried. The dried doped powders were submitted to various thermal pre-treatments, to induce chloride decomposition as well as solid-state reaction to yield the final phases.

X-ray diffraction analyses were performed on powders calcined at 600 °C for 0.1 h, at 900, 1150 and 1300 °C for 0.5 h and at 1450 °C for 2 h to follow the phase evolution. However, probably due to the low volume percentage of the YAG phase (5 vol.%) in the composite powders, it was not possible to clearly follow the new phase formation by XRD, in particular for the low-temperature treated powders. For this reason, a Y-doped NanoTek material, having a final composition corresponding to 80 vol.% Al_2O_3–20 vol.% YAG (AY80), was also prepared with the aim of overcoming the above limitation.

Taimei alumina was firstly dispersed under magnetic stirring for 96 h, and then post-doped by testing two different procedures. In the first case, the same route adopted for NanoTek powder was employed. In the second one, doped Taimei was prepared by drop-wise addition of a mixed $YCl_3{\cdot}6H_2O$ and $AlCl_3{\cdot}6H_2O$ (in the molar ratio of 3:5) aqueous solution.

Doped NanoTek and Taimei powders, after spray drying, were pre-treated at 600 °C for 0.1 h prior to uniaxial pressing in bars (17 mm × 5 mm × 5 mm) at about 300 MPa and natural sintering.

The microstructures of all the composite materials were observed by using SEM (Hitachi S2300) and ESEM (FEI XL30 ESEM FEG) microscopy.

3. Results and discussion

3.1. An immiscible system: Al_2O_3–ZrO_2

As-received Taimei is characterized by agglomerates size of about 8.6, 29.5 and 66.7 μm, corresponding to 10, 50 and 90% of the cumulative volume distribution, respectively. A good deagglomeration was achieved after 96 h of magnetic stirring or even after 3 h of ball-milling. The cumulative size distributions by volume of the dispersed samples are collected in Fig. 1 and compared with that of the as-received material, showing a signif-

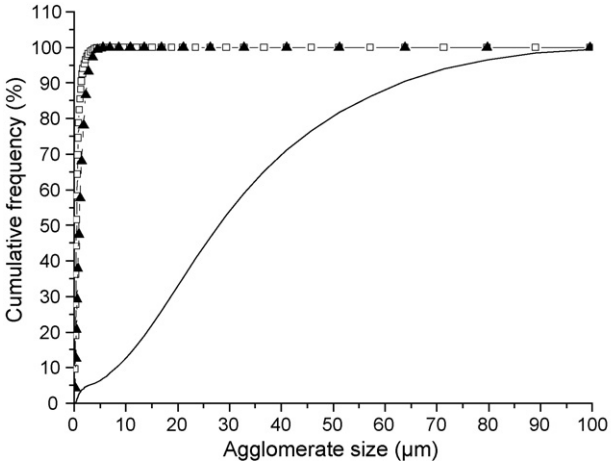

Fig. 1. Cumulative size distribution by volume of the as-received Taimei (solid line without symbols) and of the magnetically stirred (squares) and ball-milled (triangles) powder suspensions.

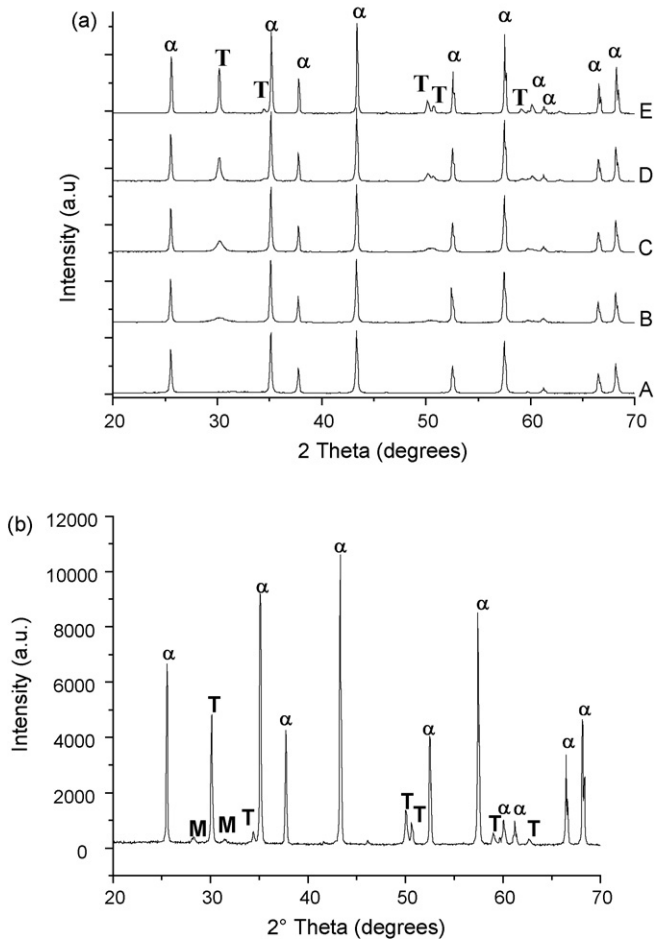

Fig. 2. (a) XRD patterns of 95 vol.% Al_2O_3–5 vol.% ZrO_2 powder calcined at (A) 400 °C, (B) 500 °C, (C) 800 °C, (D) 1200 °C and (E) 1500 °C (without soaking time). T = tetragonal ZrO_2. (b) XRD pattern of the same material calcined at 1500 °C for 3 h. T = tetragonal ZrO_2; M = monoclinic ZrO_2.

icant reduction (of about one order of magnitude) of the starting agglomerate size.

The magnetically stirred slurry was divided into two batches, one of which was doped with the zirconium chloride solution, and then oven-dried. The dried powder was calcined in the temperature range 500–1500 °C (without soaking time). From XRD analyses, tetragonal zirconia (T in Fig. 2a) started to crystallize at 500 °C and this phase remained the only one detected even after treatments at higher temperatures up to 1500 °C (Fig. 2a), although no phase stabilizers were added. On the contrary, if the soaking time at 1500 °C was prolonged up to 3 h, both monoclinic and tetragonal zirconia (T and M, respectively, in Fig. 2b) were detected. Precisely they were present in the following percentage: about 10% monoclinic and 90% tetragonal, as evaluated by the Garvie–Nicholson equation.[25]

The doped powder, calcined at 500 °C (without soaking time), and as-received Taimei, pressed in bars, were sintered in a dilatometer up to 1500 °C for 3 h (heating rate of 10 °C/min). In Fig. 3, the sintering behaviour of the doped material (solid line) is compared to that of pure Taimei powder (dashed line).

The green densities, calculated starting from weight and geometrical measurements, were 2.17 and 2.25 g/cm^3 for pure and

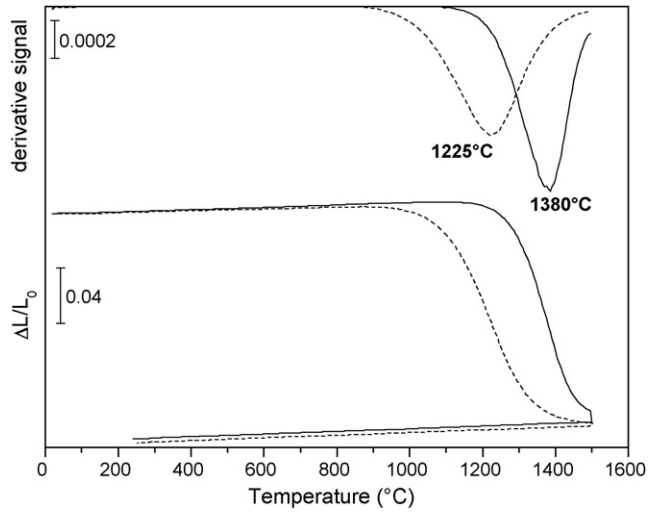

Fig. 3. Dilatometric and derivative curves of pure Taimei powder (dashed line) and of Zr-doped material (solid line) treated up to 1500 °C for 3 h.

doped samples, respectively. During sintering, they underwent a similar linear shrinkage of about 16.5%. However, the onset sintering temperature of pure alumina sample (about 1045 °C) was displaced at a significantly higher value (about 1230 °C) in the composite material, as a consequence of the dopant presence as expected from the literature data.[26]

Final densities were calculated from shrinkage data and green density, also considering weight loss: they were 94% of the theoretical value (3.97 g/cm^3) for pure Taimei and 93.7% of the theoretical density (4.06 g/cm^3) for the composite material. By XRD analysis, performed on the sintered bar, both monoclinic and tetragonal zirconia were again detected.

For improving densification, the role of the heating rate during firing was investigated. The above-doped material was sintered up to 1500 °C for 3 h, but with a heating rate of 2 °C/min in the 1100–1500 °C range. The influence of the heating rate on the sintering behaviour is negligible if compared to the effect induced by doping: however, a slight displacement (of about 35 °C) of the sintering curve to lower temperatures was observed for the low-rate fired material, so that this new heating rate was employed in the following sintering tests.

Other preliminary investigations were performed on the magnetically stirred suspensions, and precisely two different drying procedures (oven and spray drying) were compared to study their effect on green and final density, powder sinterability and fired microstructure. Bars obtained by pressing oven-dried and spray-dried powders were sintered up to 1500 °C for 3 h.

The green densities are very similar for both materials (about 2.1–2.2 g/cm^3) as well as the maximum sintering rate temperature (about 1350 °C), as shown by the derivatives curves. On the contrary, a clear difference in powder sinterability was observed, since the spray-dried sample showed an improved shrinkage in the high-temperature regime, thus reaching 96.4% of the theoretical density. Moreover, the microstructure of the oven-dried sample is characterized by a poorly homogeneous distribution of the dopant phase, as shown in Fig. 4, probably induced by the drying procedure which should induce sedimentation and sub-

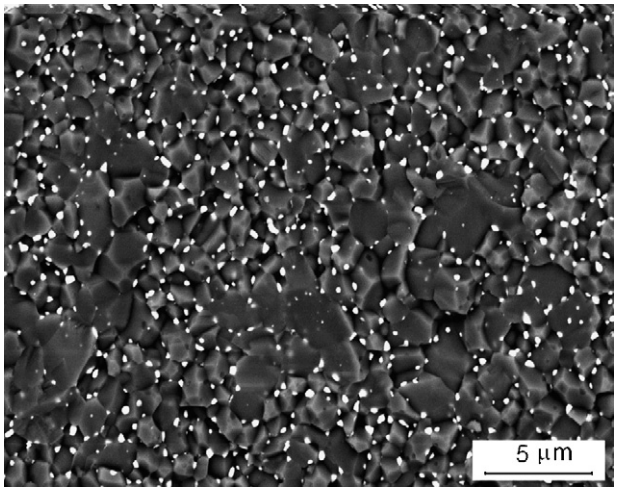

Fig. 4. Microstructure of alumina–zirconia materials from oven-dried doped powder (BSE-ESEM image).

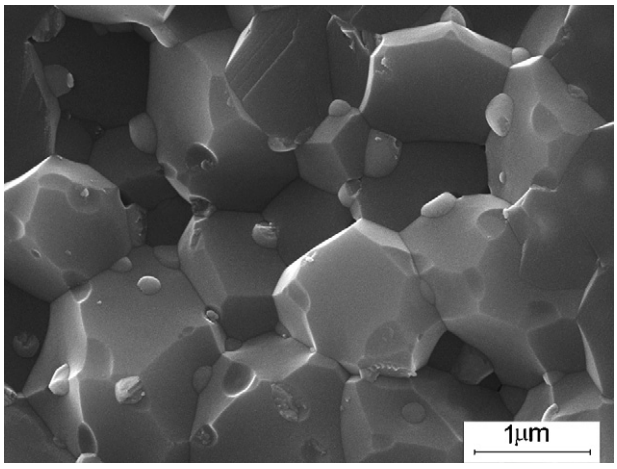

Fig. 6. High-magnification SE-ESEM image of alumina–zirconia microstructure from spray-dried doped powders.

sequent segregation between powder and doping solution. This statement is supported by the comparison to Fig. 5, in which a high homogeneity in dopant distribution was preserved by atomizing small suspension droplets. To better assess the difference in homogeneity, image analyses were performed on several SEM micrographs to find comparable microstructural descriptors. The image was divided into squared parts of 5 μm in size, and the fraction surface occupied by the zirconia grains was estimated with respect to the overall area of 25 μm^2. Normalizing these data to the higher value of zirconia fraction surface for each material, assumed equal to 1, it was possible to calculate that the variability in zirconia frequency was in the range 0.3–1 for the material obtained from the oven-dried powder, whereas in the case of materials prepared from spray-dried powders it was just between 0.6 and 1.

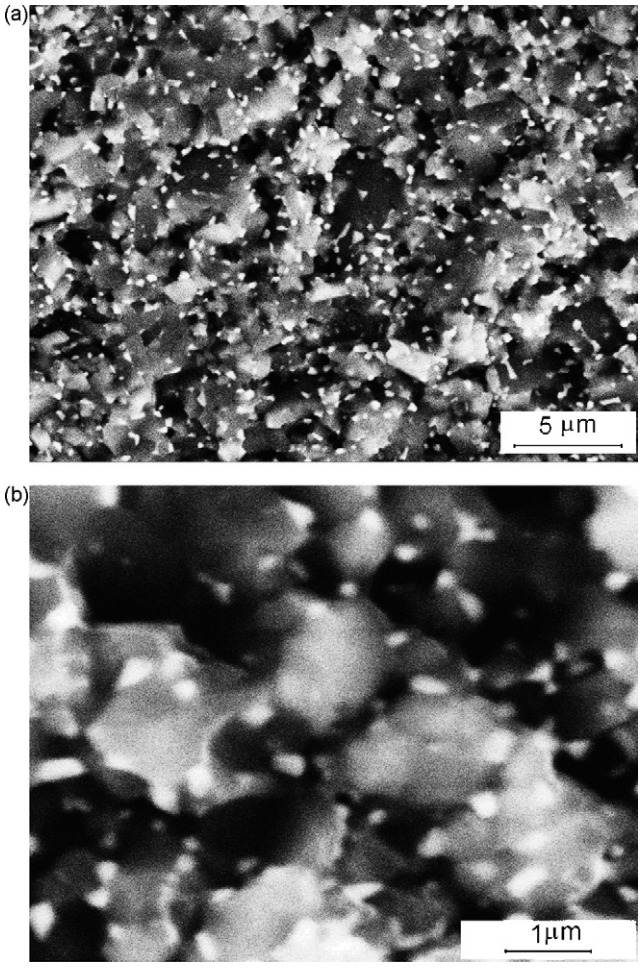

Fig. 5. Microstructure of alumina–zirconia materials from spray-dried doped powders: (a) low- and (b) high-magnification BSE-SEM image.

The high-magnification ESEM micrograph of Fig. 6, performed on the material obtained from spray-dried doped powder, allows to appreciate a very homogeneous and fine distribution of zirconia grains in both inter- and intra-granular positions. The size of the zirconia grains ranges between 250 and 300 nm.

Finally, the influence of the dispersion method (stirring or ball-milling) on the sintering behaviour was investigated. The doped powders derived from the two dispersion processes behaved similarly, since they reach almost the same green (about 2.1 g/cm^3) and fired (95.8–96.4% d_{th}) densities and their dilatometric curves are quite superimposable. Therefore, it clearly appears that the two dispersion processes are quite equivalent, thus ball-milling, requiring a relevantly shorter dispersion time, should be preferred to magnetical stirring.

3.2. A reactive system: Al_2O_3–YAG

For the dispersion of Taimei powder, the previously described experiences were exploited.

Concerning the transition alumina powder, as-received NanoTek is characterized by agglomerates size of about 1.7, 5.5 and 10.4 μm, corresponding to 10, 50 and 90% of the cumulative volume distribution. This material was dispersed under magnetic stirring for about 120 h or by ball-milling for 2.5 h, in order to reach similar particle size distributions. In Fig. 7, the cumulative size distributions by volume of the dispersed samples are compared to that of the as-received material.

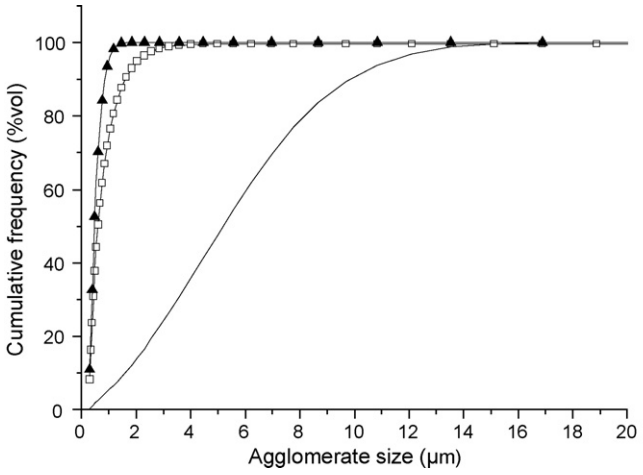

Fig. 7. Cumulative size distribution by volume of the as-received NanoTek (solid line without symbols) and of the magnetically stirred (squares) and ball-milled (triangles) powder suspensions.

NanoTek dispersed suspensions were then doped with an yttrium chloride aqueous solution to prepare a 95 vol.% Al_2O_3–5 vol.% YAG (AY95) composite powder.

A magnetically stirred slurry was also divided into two batches, one of which was doped, and then oven-dried. The doped powder was also calcined at 600 °C for 0.1 h. Both powders were pressed in bars and then sintered into a dilatometer up to 1500 °C for 3 h. Their sintering behaviour are compared in Fig. 8.

AY95 shows a significant increase of the onset sintering temperature (from about 1040 °C to about 1150 °C), similarly to the behaviour of Zr-doped samples (see Fig. 3), and already reported in the literature.[12,16,27] A two-step sintering behaviour was observed for both samples, attributable to the phase transformation from transition to α-alumina and to α-phase sintering.[20,28] The peak on the derivative curve corresponds to the temperature of maximum rate of transformation phenomena, during the first sintering step. It is located at 1145 and 1227 °C for pure and doped samples, respectively.

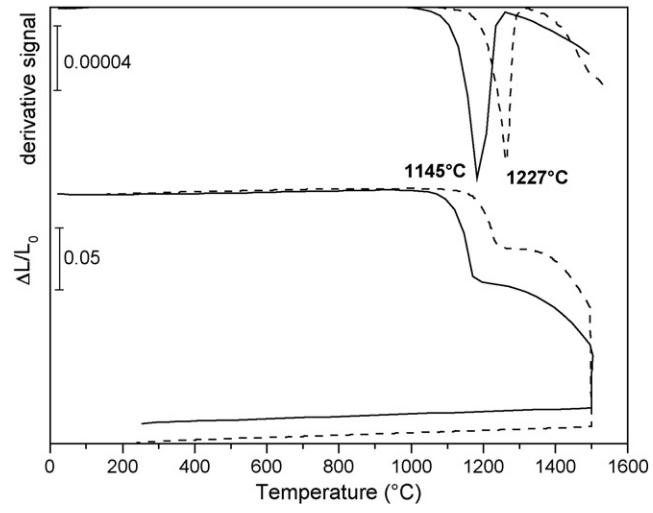

Fig. 8. Dilatometric and derivative curves of pure NanoTek powder (solid line) and of the Y-doped material (dashed line) up to 1500 °C for 3 h.

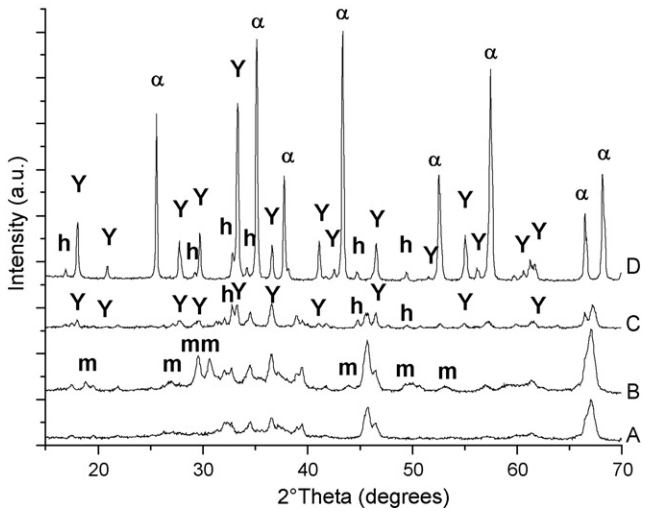

Fig. 9. XRD patterns of AY80 powder calcined at (A) 600 °C for 0.1 h, (B) 900 °C for 0.5 h, (C) 1150 °C for 0.5 h and (D) 1300 °C for 0.5 h (α = α-Al_2O_3, m = YAM; Y = YAG, h = h-$YAlO_3$).

To investigate yttrium aluminates crystallization during heat treatments, both AY95 and AY80 powders were calcined in the temperature range 600–1450 °C and submitted to XRD analyses. In Fig. 9, the XRD patterns of AY80, after calcination at 600 °C for 0.1 h, 900, 1150 and 1300 °C for 0.5 h, are reported. After calcination at 600 °C, only transition alumina was detected. Crystallization of yttrium aluminates starts at 900 °C with the formation of monoclinic $Y_4Al_2O_9$ (YAM, labelled as m in Fig. 9). It transforms at 1150 °C yielding a mixture of YAG and metastable, hexagonal $YAlO_3$ (h-$YAlO_3$, labelled as h in Fig. 9). In addition to the yttrium aluminates, only transition alumina was identified. After calcination at 1300 °C, the predominant phases were YAG and α-Al_2O_3 (respectively labelled as Y and α in Fig. 9), near traces of h-$YAlO_3$. Calcination treatment at 1450 °C for 2 h allowed to produce a mixture of well-crystallized YAG and α-alumina.

In AY95 powders, only transition aluminas were determined by XRD on samples calcined in the 600–1150 °C range. After calcination at 1300 °C for 0.5 h, YAG, α-Al_2O_3 and traces of orthorhombic $YAlO_3$ were determined; finally, after treating at 1450 °C for 2 h, also AY95 yielded a mixture of well-crystallized YAG and α-Al_2O_3 (respectively labelled as Y and α in Fig. 10), as reported in.

On the ground of XRD results, it can be supposed that transition alumina transformation to α-phase as well as crystallization of yttrium aluminates and subsequent conversion into YAG phase are associated to the first shrinkage step. The second-step is mostly related to the densification of the composite material.

In addition, the influence of the AY95 pre-treatment temperature on the sintering behaviour was investigated, by studying materials calcined at 600 °C (for 0.1 h), 900 °C (for 0.5 h) and 1150 °C (for 0.5 h).

The green densities are affected by the calcination temperature, since the values of 1.98, 1.75 and 1.69 g/cm^3 were measured for samples pre-treated at 600, 900 and 1150 °C, respectively. These differences could be imputed to different compaction behaviour during pressing. The high-temperature treated pow-

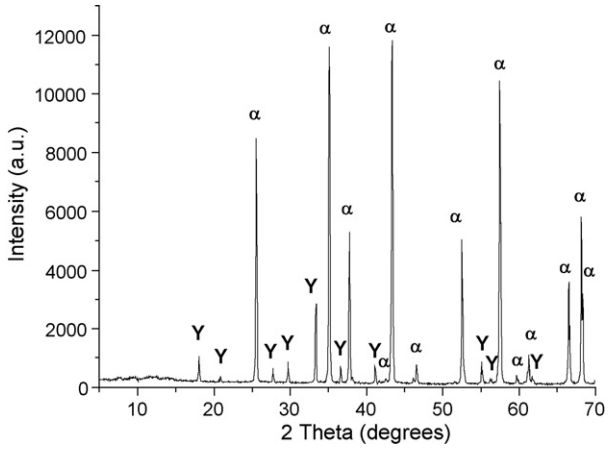

Fig. 10. XRD pattern of AY95 powder calcined at 1450 °C for 2 h (α = α-Al_2O_3, Y = YAG).

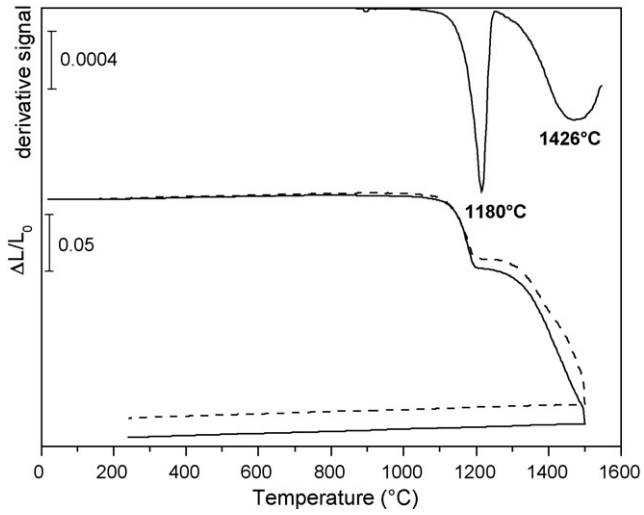

Fig. 11. Dilatometric and derivative curves of doped NanoTek powder, after dispersion by performing 2.5 h of ball-milling (solid line), sintered up to 1500 °C for 3 h (heating rate of 1 °C/min in the 700–1500 °C temperature range). As a comparison, the dilatometric curve (dashed line) of the magnetically stirred material is reported.

ders present a less effective particle packing, probably induced by a more relevant hard agglomeration with increasing pre-treatment temperature.

The differences in green densities lead to different linear shrinkages: in particular, it is significantly lower for the 600 °C pre-treated powder (about 19.8%) as compared with the high-temperature treated materials (about 22.9%). To calculate the final fired densities, it must be also considered that the three materials underwent different residual mass loss during firing up to 1500 °C. In particular, mass loss of 2.5, 1.8 and 1.2% were recorded for samples pre-treated at 600, 900 and 1150 °C, respectively, yielding final densities of 93.9, 93.3 and 91.3% of the theoretical value (3.99 g/cm^3).

In addition, the powder treated at 1150 °C presented a slighter shrinkage associated to the first-step, but it is completely recovered in the second one. However, the most significant difference was the larger linear shrinkage of samples pre-treated at 900 and 1150 °C in the second-step and during the isothermal soaking time. Thus, the pre-crystallization of yttrium aluminates in the starting powder seems to be effective in enhancing densification.

The sintering behaviour of doped NanoTek powders was investigated as a function of the heating rate, which was lowered to 1 °C/min in the temperature range 700–1500 °C, at which the main phenomena involved during thermal treatments (namely crystallization of yttrium aluminates, transition alumina particle rearrangement and transformation to α-phase, and densification) are associated. Both pressed bodies presented a green density of about 2 g/cm^3, and they underwent a similar shrinkage during sintering, reaching a final density of about 95% of the theoretical value. However, the lowering of the onset temperature (at about 1100 °C) as well as a more relevant shrinkage during the second shrinkage step were clearly observed in the material sintered at 1 °C/min.

To reduce the time of dispersion of the NanoTek powders prior to doping, a ball-milling procedure was set-up in order to achieve a comparable particle size distribution. The dilatometric curve of a pressed bar of the above powder, recorded by using a heating rate of 1 °C/min in the temperature range 700–1500 °C, is presented in Fig. 11 (solid line), and compared to that of a magnetically stirred doped sample (dashed line). The ball-milled material presents an increased linear shrinkage, which is almost completed during the heating step. The final density of the ball-milled material was about 3.97 g/cm^3, corresponding to 99.5% of the theoretical value; its derivative curve, reported in the same figure, shows that the maximum sintering rate occurred at about 1425 °C. As a consequence, a ball-milled, doped material was also sintered up to 1450 °C for 3 h, reaching a final density of about 95% of the theoretical density.

Concerning Taimei powder, a batch was dispersed under magnetic stirring for 96 h and then doped. After thermal treatment at 600 °C for 0.1 h, it was pressed in bars and then sintered up to 1500 °C for 3 h, by applying a low heating rate (2 °C/min) in the temperature range 1100–1500 °C, on the ground of previous results on the Zr-doped Taimei.

The green density was 2.1 g/cm^3, and after sintering, almost the theoretical value was reached. In addition, the maximum sintering rate occurred at about 1380 °C, thus allowing sintering with a maximum temperature in the range 1400–1450 °C. Full densification (about 99.7% of the theoretical density) was again obtained by sintering at 1450 °C for 3 h.

XRD analysis performed on Y-doped Taimei powder calcined at 1450 °C for 30 min, revealed the appearance of traces of secondary stable phases, namely orthorhombic-$YAlO_3$ perovskite (YAP) and monoclinic $Y_4Al_2O_9$ (YAM), near the expected YAG and α-Al_2O_3 (respectively labelled as P, m, Y and α in Fig. 12, curve B), as better detailed in a previous paper.[29] However, by heat treating at 1500 °C for 3 h, an almost pure alumina–YAG composite was yielded. A doped Taimei powder, produced by the addition of a dopant solution containing both Al and Y chlorides, was also calcined at 1450 °C for 0.5 h, and submitted to XRD. In this case, a composite powder purely made of YAG and α-Al_2O_3 was yielded (respectively labelled as Y and α in Fig. 12, curve A), thus denoting that this second doping route could represent an effective approach, to be exploited

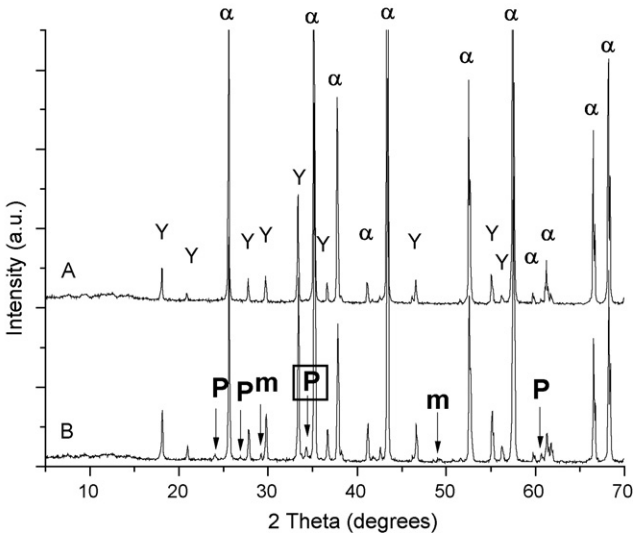

Fig. 12. XRD patterns of Taimei doped powder, calcined at 1450 °C for 0.5 h: (A) Y- and Al-doped Taimei (Y = YAG, α = α-Al_2O_3) and (B) Y-doped Taimei (Y = YAG α = α-Al_2O_3, P = orthorhombic $YAlO_3$, m = monoclinic $Y_4Al_2O_9$).

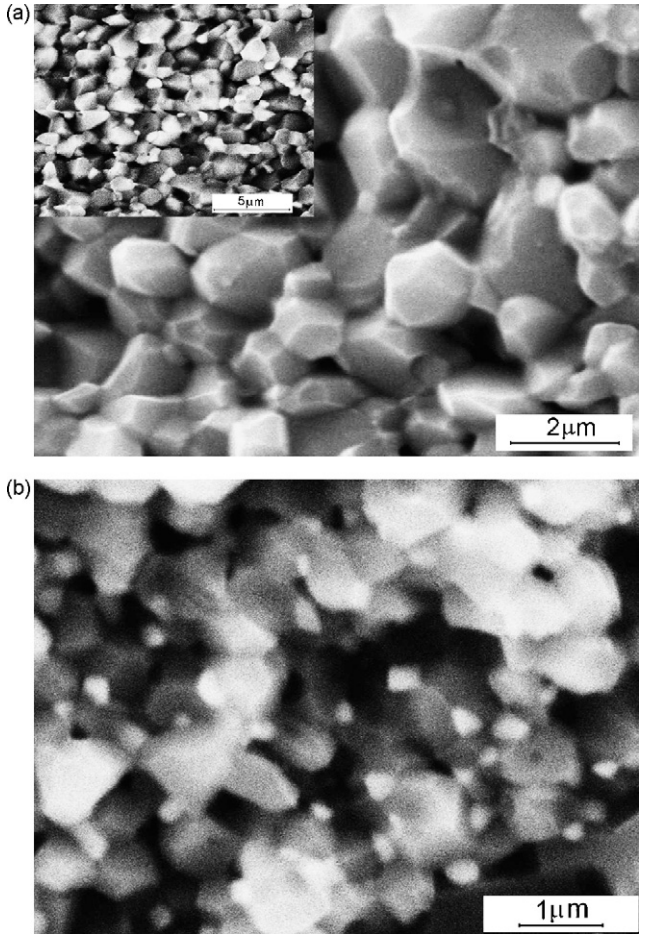

Fig. 13. SEM micrographs of doped-NanoTek materials, sintered at (a, SE image) 1500 °C and (b, BSE image) 1450 °C for 3 h. The insert of (a) is a BSE image.

in future tests, for improving the final purity of the composite material.

Selected doped NanoTek and doped Taimei sintered samples were submitted to SEM/ESEM observations, performed on fracture surfaces. In Fig. 13a, the microstructure of doped NanoTek, sintered at 1500 °C for 3 h, is reported, showing a highly dense microstructure, made of well-facetted alumina grains of about 1 μm in size. The BSE-SEM image in the insert makes it possible to observe the YAG particles, having a mean grain size of about 500 nm, homogeneously located in the alumina matrix, mostly at inter-granular positions. The lowering of the maximum sintering temperature to 1450 °C for 3 h, resulted in a refinement of the above microstructure (Fig. 13b), in spite of a slight decrease of the fired density. The BSE-SEM image shows a highly homogeneous microstructure, made of well-facetted alumina grains of about 1 μm in size and of a well-distributed equiaxial YAG particles with a mean size of about 300 nm.

In Fig. 14a, the microstructure of doped Taimei samples, sintered at 1500 °C for 3 h, is reported. The material presents a homogeneous microstructure made of well-facetted α-alumina grains of few microns in size, whereas almost spherical grains of YAG having a mean size of about 250 nm are located in both inter- and intra-granular positions. A similar microstructure, even if slightly finer, was observed in the material sintered at 1450 °C for 3 h (Fig. 14b), in which YAG grains,

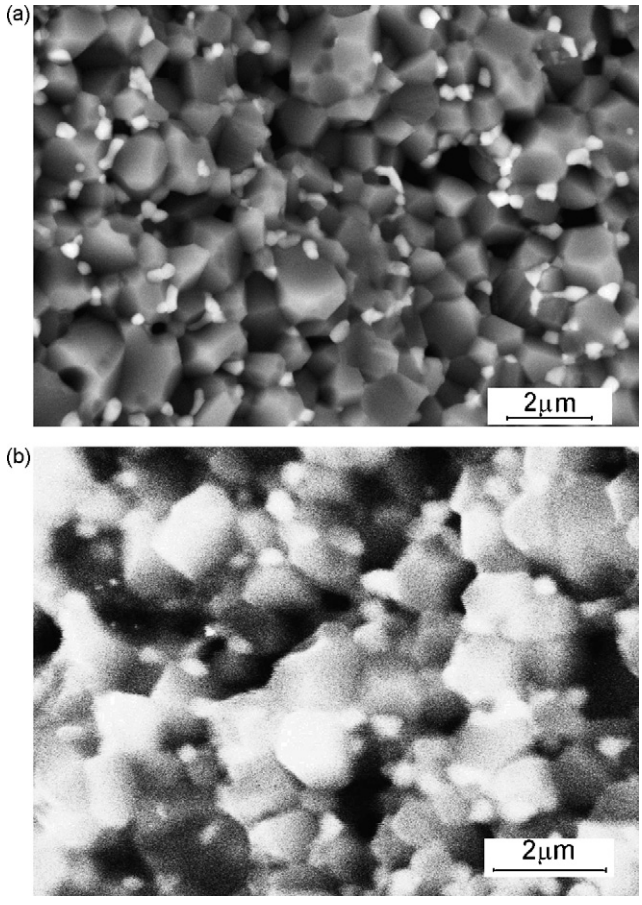

Fig. 14. Micrographs of doped Taimei materials sintered at 1500 °C (a, BSE-ESEM image) and 1450 °C (b, BSE-SEM image) for 3 h.

mostly located at inter-granular positions, have a size of about 200–300 nm.

4. Conclusions

This research has demonstrated that post-doping of commercial, both transition and α-alumina powders by using yttrium or zirconium oxide inorganic precursors should be successfully exploited to produce very fine and homogeneous YAG–alumina and ZrO_2–alumina dense composites. Therefore, this route is an effective alternative to the preparation of composite starting powders by using, for instance, reverse-strike co-precipitation. By controlling some crucial process parameters, such as alumina powder dispersion route, post-doping procedure and subsequent drying step, sintering cycle and particularly heating rate, it is possible to refine the obtained microstructure towards the preparation of micro-nanocomposite materials.

Acknowledgments

The authors wish to thank the European Commission and the Italian Ministry MIUR to have partially supported this research in the framework of the IP project NANOKER and of the project Legge 449/97 "Materiali compositi per applicazioni strutturali di rilevante interesse industriale".

References

1. Hirvonen, A., Nowak, R., Yamamoto, Y., Sekino, T. and Niihara, K., Fabrication, structure, mechanical and thermal properties of zirconia-based ceramic nanocomposites. *Journal of the European Ceramic Society*, 2006, **26**, 1497–1505.
2. Sternitzke, M., Structural ceramic nanocomposites. *Journal of the European Ceramic Society*, 1997, **17**, 1061–1082.
3. Jeong, Y. K. and Niihara, K., Microstructure and mechanical properties of pressureless sintered Al_2O_3/SiC nanocomposites. *Nanostructured Materials*, 1997, **9**, 193–196.
4. Palmero, P., Simone, A., Esnouf, C., Fantozzi, G. and Montanaro, L., Comparison among different sintering routes for preparing alumina–YAG nanocomposites. *Journal of the European Ceramic Society*, 2006, **26**, 941–947.
5. Jin, X. H. and Gao, L., Microstructure and mechanical properties of $NdAlO_3/Al_2O_3$ nanocomposites. *Materials Science and Engineering A*, 2003, **354**, 326–330.
6. Wu, Y. Q., Zhang, Y. F., Wang, S. W. and Guo, J. K., In-situ synthesis of roadlike $LaAl_{11}O_{18}$ in Al_2O_3 powder by a coprecipitation method. *Journal of the European Ceramic Society*, 2001, **21**, 919–923.
7. Li, W. Q. and Gao, L., Processing, microstructure and mechanical properties of 25 vol.% YAG–Al_2O_3 nanocomposites. *Nanostructured Materials*, 1999, **11**, 1073–1080.
8. Wang, H. Z., Gao, L., Gui, L. H. and Guo, J. K., Preparation and properties of intergranular Al_2O_3–SiC nanocomposites. *Nanostructured Materials*, 1998, **10**, 947–953.
9. Schehl, M., Díaz, L. A. and Torrecillas, R., Alumina nanocomposites from powder–alkoxide mixtures. *Acta Materialia*, 2002, **50**, 1125–1139.
10. Torrecillas, R., Schehl, M., Díaz, L. A., Menéndez, J. L. and Moya, J. S., Creep behaviour of alumina/YAG nanocomposites obtained by a colloidal processing route. *Journal of the European Ceramic Society*, 2007, **27**, 143–150.
11. Deville, S., Chevalier, J., Fantozzi, G., Bartolomé, J. F., Requena, J., Moya, J. S. *et al.*, Low-temperature ageing of zirconia-toughened alumina ceramics and its implications in biomedical implants. *Journal of the European Ceramic Society*, 2003, **23**, 2975–2982.
12. Voytovych, R., Mac Laren, I., Gülgün, M. A., Cannon, R. M. and Rühle, M., The effect of yttrium on densification and grain growth in α-alumina. *Acta Materialia*, 2002, **50**, 3453–3463.
13. Loudjani, M. K. and Haut, C., Influence of the oxygen pressure on the chemical state of yttrium in polycrystalline α-alumina: relation with microstructure and mechanical toughness. *Journal of the European Ceramic Society*, 1996, **16**, 1099–1106.
14. Gruffel, P. and Carry, C., Effect of grain size of yttrium grain boundary segregation in fine-grained alumina. *Journal of the European Ceramic Society*, 1993, **11**, 189–199.
15. McCune, R. C., Donlon, W. T. and Ku, R. C., Yttrium segregation and YAG precipitation at surfaces of yttrium-doped α-Al_2O_3. *Journal of the American ceramic Society*, 1986, **69**, 196c–199.
16. Cinibulk, M. K., Effect of yttria and yttrium–aluminum garnet on densification and grain growth of alumina at 1200–1300 °C. *Journal of the American Ceramic Society*, 2004, **87**, 692–695.
17. Lartigue, S., Priester, L., Dupau, F., Gruffel, P. and Carry, C., Dislocation activity and differences between tensile and compressive creep of yttria doped alumina. *Materials Science and Engineering A*, 1993, **164**, 211–215.
18. Cawley, J. D. and Halloran, J. W., Dopant distribution in nominally yttrium-doped sapphire. *Journal of the American Ceramic Society*, 1986, **69**, C-195-C-196.
19. Loudjani, M. K., Foy, J. and Haut, C., Study by extended X-ray absorption fine-structure technique and microscopy of the chemical state of yttrium in α-polycrystalline alumina. *Journal of the American Ceramic Society*, 1985, **68**, 559–562.
20. Legros, C., Carry, C., Bowen, P. and Hofmann, H., Sintering of a transition alumina: effects of phase transformation, powder characteristics and thermal cycle. *Journal of the European Ceramic Society*, 1999, **19**, 1967–1978.
21. Dynys, F. W. and Halloran, J. W., Alpa alumina formation in alum-derived gamma alumina. *Journal of the American Ceramic Society*, 1982, **65**, 442–448.
22. http://www.taimei-chem.co.jp.
23. http://www.nanophase.com.
24. Azar, M., Palmero, P., Lombardi, M., Garnier, V., Montanaro, L., Fantozzi, G. *et al.*, Effect of particle packing on the sintering of nanostructured transition alumina. *Journal of the European Ceramic Society*, 2008, **28**, 1121–1128.
25. Garvie, R. C. and Nicholson, P. S., Phase analysis in zirconia systems. *Journal of the American Ceramic Society*, 1972, **55**, 303–305.
26. Lange, F. F. and Hirlinger, M. M., Hindrance of grain growth in Al_2O_3 by ZrO_2 inclusions. *Journal of the American Ceramic Society*, 1984, **67**, 164–168.
27. Fang, J., Thompson, A. M., Harmer, M. P. and Chan, H. M., Effect of yttrium and lanthanum on the final-stage sintering behaviour of ultrahigh-purity alumina. *Journal of the American Ceramic Society*, 1997, **80**, 2005–2012.
28. Bowen, P., Carry, C., Hofmann, H. and Legros, C., Phase transformation and sintering of γ-Al_2O_3: effect of powder characteristics and dopants (Mg or Y). *Key Engineering Materials*, 1997, **132–136**, 904–907.
29. Palmero, P. and Montanaro, L., Processing and sintering of alumina–YAG nanocomposites. *Advances in Science and Technology*, 2006, **45**, 1696–1703.